INTERNATIONAL JOURNAL OF PHARMACEUTICAL SCIENCES
[ISSN: 0975-4725; CODEN(USA): IJPS00]
Journal Homepage: https://www.ijpsjournal.com

OPEN ACCESS

Research Article

In Silico Design, Synthesis, Characterization and Bioactivity Profiling of Dihydropyrimidine-2-Thione Derivatives

Nivea Cleo Ts[1*], Sreena K.[2], Fathima Rifa P.[3], Fathima CT[4], Fathimath Rasha Vv[5], Akshaya Gp[6]

[1] Associate Professor, Department of Pharmaceutical Chemistry, Crescent College of Pharmaceutical Sciences, Payangadi P O, Kannur-670358, Kerala, India, 670358.
[2] Professor and HOD, Department of Pharmaceutical Chemistry, Crescent College of Pharmaceutical Sciences, Payangadi P O, Kannur-670358, Kerala, India, 670358.
[3,4,5] Department of Pharmaceutical Chemistry, Crescent College of Pharmaceutical Sciences Payangadi P O, Kannur-670358, Kerala, India, 670358.
[6] Associate Professor, Department of Pharmaceutical Chemistry, Crescent College of Pharmaceutical Sciences, Payangadi P O, Kannur-670358, Kerala, India, 670358.

ARTICLE INFO

Published: 27 Nov 2026
Keywords:
Dihydropyrimidine-2-thione derivatives, Biginelli reaction, HRBC membrane stabilization assay, MTT assay
DOI:
10.5281/zenodo.24578615

ABSTRACT

Bioactivity profiling of dihydropyrimidine-2-thione (DHPMT) derivatives was carried out to evaluate their potential anti-inflammatory and anticancer activities using computational and experimental approaches. Molecular docking studies were performed against cyclin-dependent kinase 2 (CDK2; PDB ID: 1KE9) and phospholipase A2 (PDB ID: 1ZYX) using AutoDock Vina .DHPT1 exhibited a highest docking score of -7.5 kcal/mol against CDK2 and DHPT2 showed the highest docking score of -7.8 kcal/mol against PLA2 indicating favourable predicted binding affinities followed by in-silico ADME and toxicity predictions. The selected derivatives, DHPT1 and DHPT2, were synthesized using the Biginelli multicomponent reaction and characterized by TLC, melting point determination, FTIR and NMR spectroscopy. *In-vitro* anti-inflammatory activity was evaluated using the human red blood cell (HRBC) membrane stabilization assay, with indomethacin as the reference standard. DHPT2 exhibited greater membrane stabilization (71.57%) with an IC_{50} value of 18.20 µg/ml. DHPT1 was further evaluated against MCF-7 breast cancer cells using the MTT assay, showing 62.97% cell viability at 100 µg/ml.

***Corresponding Author:** Nivea Cleo Ts
Address: Associate Professor, Department of Pharmaceutical Chemistry, Crescent College of Pharmaceutical Sciences, Payangadi P O, Kannur-670358, Kerala, India, 670358.
Email : niveacleots@gmail.com

Relevant conflicts of interest/financial disclosures: The authors declare that the research was conducted in the absence of any commercial or financial relationships that could be construed as a potential conflict of interest.

INTRODUCTION

Breast cancer is one of the most commonly diagnosed malignancies among women worldwide and represents a major public health concern. It is influenced by genetic, hormonal and environmental factors. Alterations in genes such as BRCA1, BRCA2 and TP53, along with dysregulation of cellular signalling pathways, contribute to breast cancer development and progression. Abnormal activation of pathways such as PI3K/AKT and RAS/MEK/ERK can promote uncontrolled cellular proliferation, tumour survival and resistance to apoptosis. These molecular changes contribute to tumour progression and therapeutic resistance.[1,2]

MCF-7 is a widely used human breast adenocarcinoma cell line derived from the pleural effusion of a patient with metastatic breast cancer. It is an estrogen receptor-positive and hormone-responsive cell line that retains several characteristics of mammary epithelial cells. Due to its estrogen receptor expression and well-established growth characteristics, MCF-7 cells serve as an important in-vitro model for investigating breast cancer biology and evaluating the anticancer potential of newly developed compounds.[3,4]

Inflammation is a protective biological response initiated by the body following tissue injury, infection or exposure to harmful stimuli. It involves vascular changes and immune cell recruitment. It is classified into acute and chronic inflammation associated with persistent inflammatory activity and tissue damage.[5,6] Inflammatory pathways such as NF-κB, COX-2, iNOS and MAPK regulate the release of pro-inflammatory cytokines such as TNF-α, IL-1β and IL-6. Persistent activation of inflammatory pathways may contribute to chronic inflammatory disorders and several pathological conditions, including cardiovascular diseases, diabetes and cancer.[7,8]

Dihydropyrimidines (DHPMs) are six-membered nitrogen-containing heterocyclic compounds characterized by a partially saturated pyrimidine ring. These compounds are commonly synthesized through the Biginelli multicomponent reaction, involving the condensation of an aldehyde, a β-ketoester and urea or thiourea.[9,10] Among the structural modifications of DHPMs, replacement of the carbonyl group at the second position (C=O) with a thiocarbonyl group (C=S) results in the formation of dihydropyrimidine-2-thiones (DHPMTs). These compounds has been investigated for various pharmacological activities, including anticancer, anti-inflammatory, antibacterial, antiviral, antioxidant and cytotoxic effects. The introduction of sulfur in place of oxygen may influence the physicochemical properties, intermolecular interactions and biological activity of the resulting derivatives.[11] In this context, the present study focuses on the in-silico design, synthesis, characterization and bioactivity profiling of dihydropyrimidine-2-thione derivatives.

MATERIALS AND METHODS

2.1. MATERIALS

The chemicals and reagents used in the study were procured from Sigma-Aldrich, Alchemy Lab solutions, Edapally Kochi. The melting point were determined by open capillary method. IR spectra were recorded on Perkins Elmer FTIR spectrophotometer, and values are expressed in cm^{-1}. ^{1}H NMR (at 400 MHz) and ^{13}C-NMR (101 MHz) spectra were recorded on JEOL FT-NMR spectrophotometer (JSS College of Pharmacy, SS Nagar, Mysore, Karnataka) and the chemical shifts are reported in parts per million (δ value), with TMS (δ 0 ppm for ^{1}H NMR) used as the internal standard.

2.2 *IN-SILICO* STUDY

All computational analysis was carried out on a Windows 10 Pro OS platform on a Desktop with an Intel (R) Pentium (R) CPU J3710 @ 1.60GHz and 4 GB RAM.

2.3 PHARMACOKINETIC STUDY BY SWISSADME

SwissADME is a freely accessible web-based tool used to predict physiochemical properties (Molecular weight, Molar refractivity, Polar surface area), pharmacokinetics (substrate or non-substrate of P- gp, CYP inhibition), drug-likeness of potent molecule. It also provides predictive models, such as boiled egg allows the evaluation of human intestinal absorption (HIA) and brain penetration (BBB) of drug molecule. The white region is for high probability of passive

absorption by the GI tract and yolk region is for high probability of brain penetration.[12]

Lipinski's rule of five

Lipinski's rule is a tool to access ADME properties and predict drug-likeness. The rule shows the following extensions:

- Not more than 5 hydrogen bond donors (the total number of nitrogen–hydrogen and oxygen hydrogen bonds)
- Not more than 10 hydrogen bond acceptors (all nitrogen or oxygen atoms)
- Molecular mass should be less than 500 Daltons
- Octanol-water partition coefficient (log P) should not exceed 5.[13]

2.4 *IN-SILICO* TOXICITY PREDICTION – PROTOX.3.0

In silico toxicity prediction was performed using ProTox-3.0. It is a free software available for access in the Organic Chemistry Portal. Using this prediction tool mutagenicity, tumorigenicity, skin irritation and reproductive effects can be calculated.

Toxicity classes are defined according to the globally harmonized system of classification of labelling of chemicals (GHS). LD50 values are given in [mg/kg]:

Class I: Fatal if swallowed (LD50≤)

Class II: Fatal if swallowed (5<LD50≤50)

Class III: Toxic if swallowed (50<LD50≤300)

Class IV: Harmful if swallowed (300<LD50≤2000)

Class V: May be harmful if swallowed (20005000).[14]

PASS Online

Prediction of Activity Spectra for Substances (PASS) is a computer program that estimate the probable profile of biological activity of a drug- like organic compound based on its structural formula. It provides a list of predicted biological activities with estimated probabilities of being 'to be active' Pa and 'to be inactive' Pi, which may vary from zero to one.

If Pa > 0.7, the changes of finding experimental activity are rather high.

If 0.5 < Pa < 0.7, the compounds will be less similar to known pharmaceutical agents.

If Pa < 0.5, the compound found to be a new chemical class for biological activity.[15]

2.5 MOLECULAR DOCKING

Molecular docking of small molecules and compounds into the binding site of receptors and the estimation of binding affinities are important components of structure-based drug design.[16] Molecular docking is achieved by AutoDock Vina. The 3D crystallographic structure of proteins were obtained from protein data bank (PDB ID-1KE9,1ZYX).

AutoDock Vina is an open-source program offering a complete molecular viewer and graphical support for all the steps inevitable for set up and docking analysis. PyMOL produce a high-quality 3D image of protein as well as its visualization. PyRx is for docking analysis.[17,18]

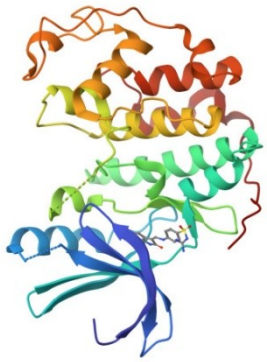

Figure 1: Protein (PDB ID:1KE9)



Figure 2: Protein (PDB ID:1ZYX)

Steps in molecular docking:

Protein preparation

Structure downloaded from PDB database is unsuitable for docking studies. Protein preparation in Biovia Discovery Studio involves cleaning, repairing, and preparing the protein structure for analysis. This may include removing unwanted molecules like water or co-factors, depending on the requirements of the docking study. Unwanted components are removed by selecting them in the Hierarchy tree view and deleting them.[16]

Ligand preparation

The 2D chemical structure of ligands are drawn using ACD Lab ChemSketch ver 12.0 or ChemDraw Ultra 12.0 and generated smiles notation. This smile notation is being converted into 3D PDB format with the help of freely accessible Online SMILES Translator.[19]

Docking using AutoDock Vina

Docking is performed in PyRX where both the derivative and receptor are loaded in navigation plane. Then the protein is converted into macromolecule and derivative into ligand molecule. After the preparation, click on AutoDock Vina Wizard start button and adjust the grid size. After the completion of process, docking value is expressed in terms of binding affinity (Kcal/mol) with RMSD upper bound and lower bound value. AutoDock Vina convert PDB to PDBQT which is followed by additional step by adding polar contacts to find out the types of amino acid interactions during ligand-receptor binding.[20]

2.6 CHEMISTRY

General procedure for the synthesis of 3,4-dihydropyrimidine-2 (1H)-thione derivative.

A mixture of thiourea (0.15 mol), ethyl acetoacetate (0.1mol) and vanillin (0.1mol) was dissolved in 20ml of ethanol in round bottom flask. 2-3 drops of hydrochloric acid were added to the reaction mixture and the mixture was refluxed for about 2 hours. The reaction mixture was then cooled and then poured into ice-cold water with stirring and kept overnight at room temperature. The resulting solid was filtered, washed with cold water and dried. The crude product was re-crystallized using ethanol. The purity of synthesized compound was determined by thin-layer chromatography (TLC).[21]

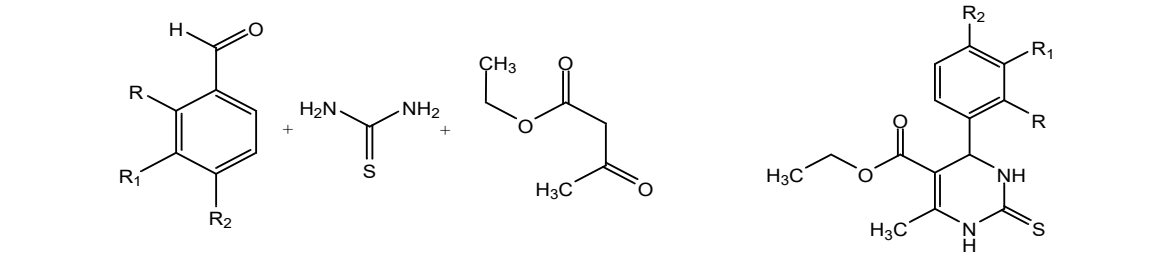

Figure 3: Synthesis of Dihydropyrimidine-2-Thione Derivatives by the Bignelli Reaction

2.7 REACTANTS

Thiourea

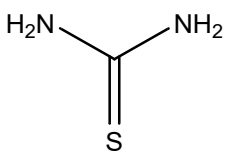

thiourea
Chemical Formula: CH_4N_2S
Molecular Weight: 76.12

Figure 4: Thiourea

Ethyl acetoacetate

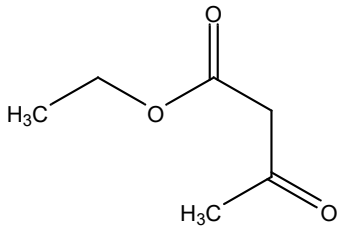

ethyl 3-oxobutanoate
Chemical Formula: $C_6H_{10}O_3$
Molecular Weight: 130.14

Figure 5: Ethyl Acetoacetate

ALDEHYDE DERIVATIVES

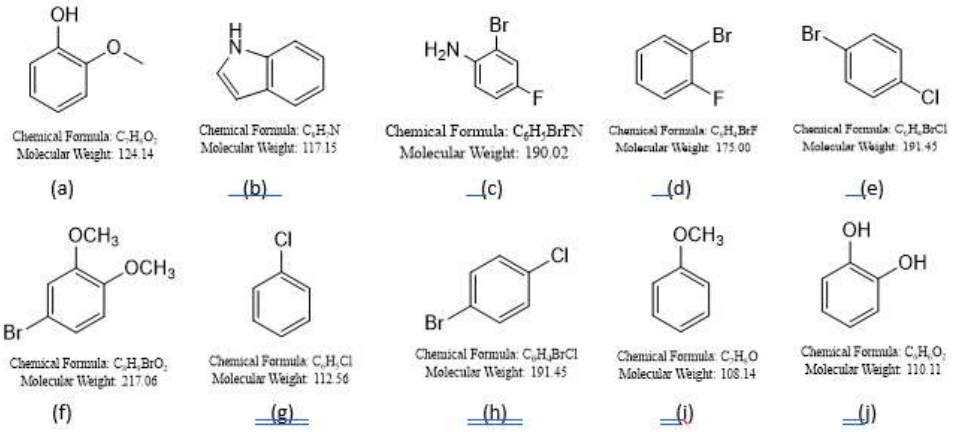

Figure 6: A) 2-Methoxyphenol, B) Indole, C) 2-Bromo-4-Fluroaniline, D) 1-Bromo-2-Fluorobenzene, E) 1-Bromo-4-Chlorobenzene, F) 4-Bromo-1,2-Dimethoxybenzene, G) Chlorobenzene, H) 1-Bromo-4-Chlorobenzene, I) Anisole, J)Catechol

2.8 STRUCTURE OF SYNTHESIZED COMPOUND

DHPT1

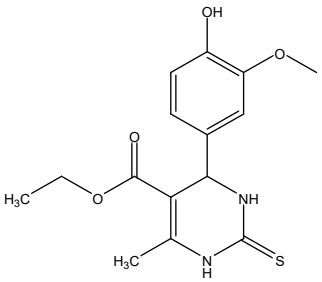

ethyl 4-(4-hydroxy-3-methoxyphenyl)-6-methyl-2-thioxo-1,2,3,4-tetrahydropyrimidine-5-carboxylate
Chemical Formula: $C_{15}H_{18}N_2O_4S$
Molecular Weight: 322.38

Figure 7: Ethyl 4-(4-Hydroxy-3-Methoxyphenyl)-6-Methyl-2-Thioxo-1,2,3,4-Tetrahydropyrimidine-5-Carboxylate

DHPT2

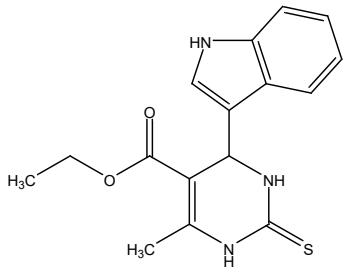

ethyl 4-(1*H*-indol-3-yl)-6-methyl-2-thioxo-1,2,3,4-tetrahydropyrimidine-5-carboxylate
Chemical Formula: $C_{16}H_{17}N_3O_2S$
Molecular Weight: 315.39

Figure 8: Ethyl 4-(1*H*-indol-3-Yl)-6-Methyl-2-Thioxo-1,2,3,4-Tetrahydropyrimidine-5-Carboxylate

2.9 CHARACTERIZATION

Melting point

The melting point of the synthesized compound was determined by open capillary tube method. The temperature at which the compound starts losing its crystallinity and changes from solid to liquid form was found and recorded.

Thin layer chromatography

The reactants and products were dissolved in DMSO. It was spotted on the TLC plate. A single principal spot for the product and the absence of secondary spots for parent compounds and intermediates confirmed the purity of the product. Stationary phase: pre-coated silica gel GF using appropriate mobile phase was used. The spots were detected in a Iodine chamber.[22]

IR spectrometry

Infrared (IR) spectroscopy is one of the most commonly used spectroscopic techniques for the identification of functional groups in molecules. It is an important tool for the structural elucidation of organic compounds. The fingerprint region of the IR spectrum is useful for comparing compounds. The IR spectrum represents percentage transmittance against frequency, expressed in wavenumbers (cm^{-1}).

NMR spectroscopy

Nuclear Magnetic Resonance (NMR) spectroscopy is an important analytical technique used for the structural elucidation of organic molecules. It involves the interaction of the electromagnetic radiation and the proton of a nucleus of an atom when placed under an externally applied static magnetic field. NMR spectra provide the detailed information about a molecule's structure. The chemical shift is used to predict the number of protons with refers to TMS as standard. The NMR spectra were recorded on JEOL FT-NMR spectrometer at 400MHz (^{13}C NMR) and 101 MHz (^{1}H NMR), with DMSO used as the solvent.[23]

2.10 BIOLOGICAL EVALUATION

In-vitro Anti-inflammatory Activity Assay:

HRBC Membrane Stabilizing Method

Principle:

The release of lysosomal enzymes during inflammation may contribute to the development of various disorders. The extracellular activity of these enzymes is associated with both acute and chronic inflammatory conditions. Non-steroidal anti-inflammatory drugs (NSAIDs) act either by inhibiting lysosomal enzymes or by stabilizing the lysosomal membrane. Since the HRBC (human red blood cell) membrane resembles the lysosomal membrane, this study was carried out to evaluate HRBC membrane stability in the presence of test samples and to predict their in-vitro anti-inflammatory activity. The compounds were tested at different concentrations and incubated separately with the HRBC suspension.

Procedure:

The Human Red Blood Cell Membrane Stabilization method (HRBC) has been used as a method to study the in-vitro anti-inflammatory activity. Blood was collected from healthy human volunteer who was not taken any NSAIDS for 2 weeks prior to the experiment. Study was commenced with due permission of the Institutional ethics committee and written consent from the subjects. The collected blood was mixed with equal volume of sterilized Alsever's solution (2% dextrose, 0.8 % sodium citrate, 0.05% citric acid and 0.42 % sodium chloride in water). The blood was centrifuged at 3000 rpm for 10 min and packed cells were washed three times with isosaline (0.85%, pH 72). The volume of the blood was measured and reconstituted as 10% v/v suspension with isosaline. The assay mixture

contains 1ml phosphate buffer [PH 7.4, 0.15 M], 2 ml hypo saline [0.36%]. 0.5 ml HRBC suspension [10 % v/v] with 0.5 ml of test sample and standard drug Indomethacine of various concentrations (10,20,50,100 µg/ml) and control (ethanol to produce 100% haemolysis) were incubated at 37°C for 30 min and centrifuged respectively. The haemoglobin content in the suspension was estimated using spectrophotometer at 560 nm.

The percentage of haemolysis of HRBC membrane can be calculated as follows:

% haemolysis = (OD of Test Sample / OD of Control) × 100

The percentage of HRBC membrane stabilization can be calculated as follows:

% Protection = 100 - [(OD of Test Sample / OD of Control)] × 100

Here "OD of test sample" is optical density or the test sample's absorbance and "OD of control" is optical density or absorbance of the negative control.

Here, the negative control used was Ethanol and it contained no Indomethacin or test sample in it.[24]

MTT assay

Principle:

The MTT assay is used to measure cellular metabolic activity as an indicator of cell viability, proliferation and cytotoxicity. This colorimetric assay is based on the reduction of a yellow tetrazolium salt (3-(4,5-dimethyl thiazole-2-yl)-2,5-diphenyltetrazolium bromide or MTT) to purple formazan crystals by metabolically active cells . The viable cells contain NAD (P)H-dependant oxido- reductase enzymes which reduce the MTT to formazan. The insoluble formazan crystals are dissolved using a solubilizing solution (100% DMSO)and the resulting purple coloured solution is quantified by measuring absorbance at 570 nm using an ELIZA plate reader.

Procedure :

The cells (10,000 cells/well) were seeded on 96 well plates and allowed to acclimatize to the culture conditions such as 37°C and 5% CO2 environment in the incubator for 24 hours. The test samples were prepared in DMSO (10 mg/mL) and filter sterilized using 0.2 µm Millipore syringe filter. The samples were further diluted in DMEM media and added to the wells containing cultured cells at final concentrations of 6.25, 12.5, 25, 50, 100 µg/mL respectively. Untreated wells were kept as control. All the experiments were done in triplicate and average values were taken in order to minimize errors. After treatment with the test samples the plates were further incubated for 24 h.

After incubation period, the media from the wells were aspirated and discarded. 100 µL of 0.5 mg/mL MTT solution in PBS was added to the wells. The plates were further incubated for 2 hours for the development of formazan crystals. The supernatant was removed and 100 µL DMSO (100%) were added per well. The absorbance at 570 nm was measured with micro plate reader. Three wells per plate without cells served as blank. All the experiments were done in triplicates.[25,26]

The cell viability was expressed using the following formula:

$$Percentage\ of\ cell\ viability = \frac{Average\ absorbance\ of\ treated}{Average\ absorbance\ of\ control} \times 100$$

RESULTS AND DISCUSSION

3.1 CHEMISTRY

The synthesized compound (DHPT1 & DHPT2) was obtained good yields (75-85%). Spectroscopic data confirmed the proposed structures.

NMR of DHPT1:

1H-NMR (400 MHz, DMSO-D6) δ 10.24 (s, 1H), 9.55 (d, J = 2.0 Hz, 1H), 8.99 (s, 1H), 6.79 (d, J = 2.0 Hz, 1H), 6.72 (d, J = 8.1 Hz, 1H), 6.59 (dd, J = 8.1, 2.0 Hz, 1H), 5.08 (d, J = 3.7 Hz, 1H), 4.05-3.98 (m, 2H), 3.73 (s, 3H), 2.28 (s, 3H), 1.12 (t, J = 7.1 Hz, 3H).

13C-NMR (101 MHz, DMSO-D6) δ 174.0, 165.3, 147.4, 146.2, 144.7, 134.6, 118.6, 115.4, 110.9, 101.0, 59.6, 55.6, 53.7, 40.1, 39.9, 39.7, 39.5, 39.3, 39.1, 38.9, 17.2, 14.1.

The ^{1}H-NMR spectrum showed signals at δ 10.24, 9.55, and 8.99 ppm corresponding to O–H and N–H protons. Aromatic protons appeared in the region of δ 6.59–6.79 ppm. The signals at δ 5.08, 4.05–3.98, 3.73, 2.28, and 1.12 ppm were attributed to the ring methine, ethyl

ester, methoxy, methyl, and ethyl methyl protons, respectively. The ^{13}C-NMR spectrum showed characteristic signals at δ 174.0 and 165.3 ppm for C=S and ester C=O carbons, respectively. Other signals supported the presence of aromatic, methoxy, and aliphatic carbons, consistent with the proposed structure.

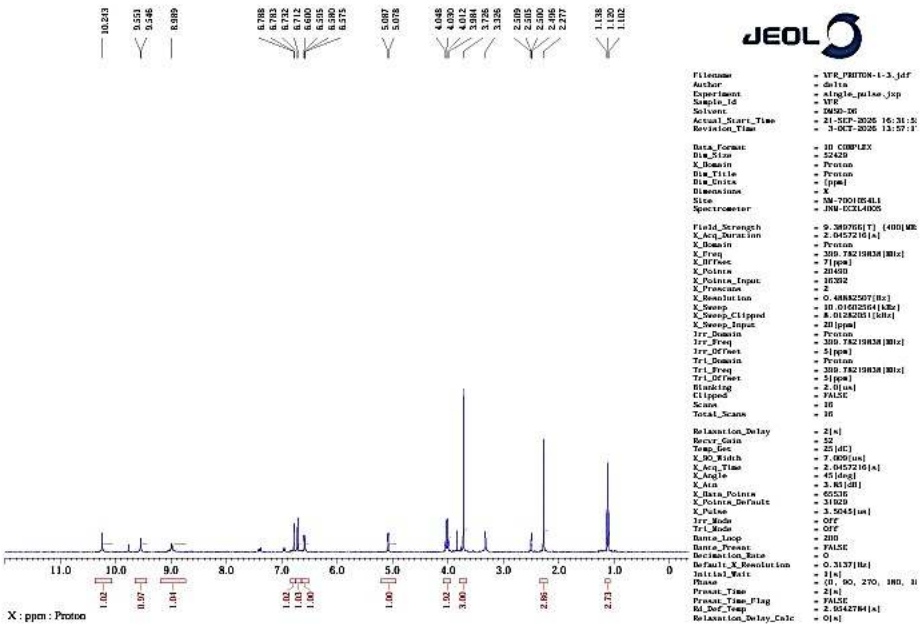

Figure 9: ^{1}H NMR Spectrum of DHPT1

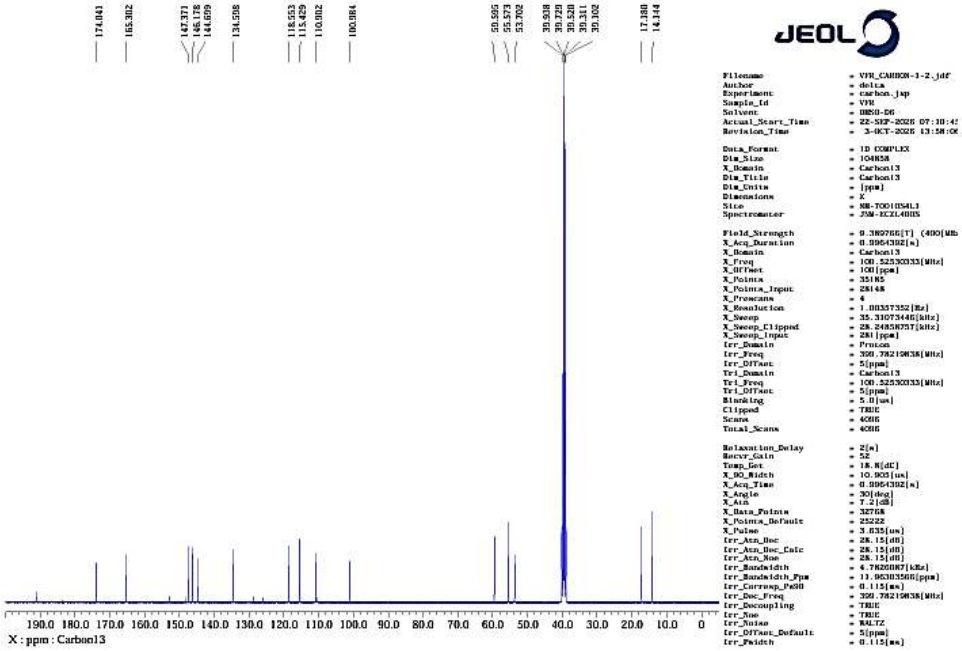

Figure 10: ^{13}C NMR Spectrum of DHPT1

NMR of DHPT2:

1H-NMR (400 MHz, DMSO-D6) δ 12.09 (s, 1H), 9.90 (s, 1H), 8.24 (d, J = 3.1 Hz, 1H), 8.05 (d, J = 8.4 Hz, 1H), 7.60-7.66 (0H), 7.48-7.46 (m, 1H), 7.24-7.16 (m, 3H)

13C-NMR (101 MHz, DMSO-D6) δ 185.0, 138.6, 137.1, 124.1, 123.5, 122.2, 120.9, 118.2, 112.5, 40.1, 39.9, 39.7, 39.5, 39.3, 39.1, 38.9.

The ^{1}H-NMR spectrum exhibited signals at δ 12.09 and 9.90 ppm, attributed to N–H protons. The signals observed in the region of δ 7.16–8.24 ppm corresponded to aromatic protons of the indole ring. The ^{13}C-NMR spectrum showed a characteristic signal at δ

185.0 ppm attributed to the thiocarbonyl (C=S) carbon. The remaining signals in the aromatic region were assigned to indole ring carbons. These spectral features supported the proposed structure of DHPT2.

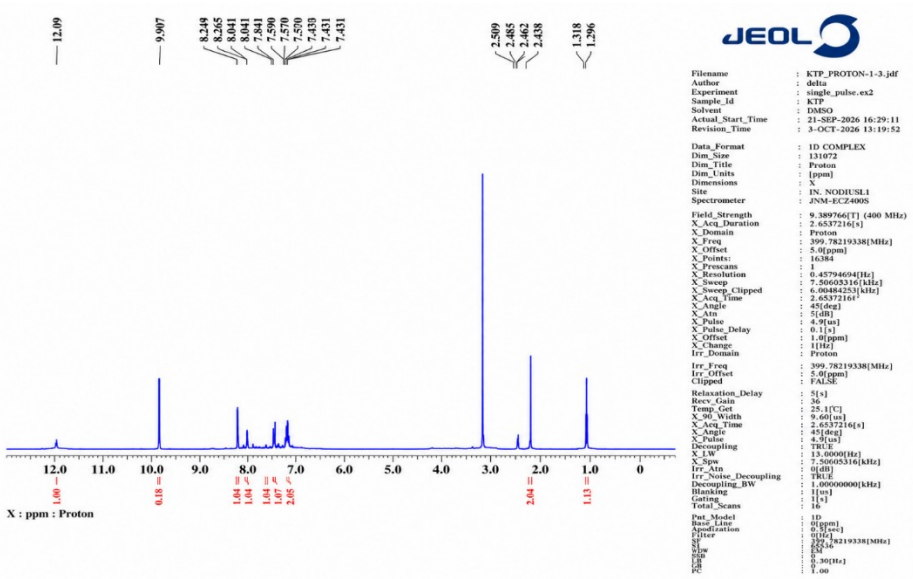

Figure 11: ^{1}H NMR Spectrum of DHPT2

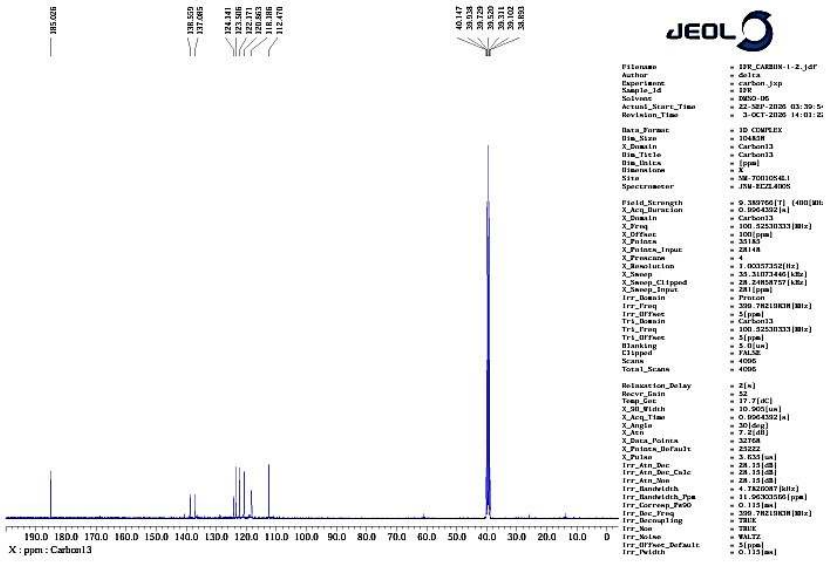

Figure 12: ^{13}C NMR Spectrum of DHPT2

IR SPECTRA

3411 (O–H), 3170 (N–H), 2998 (C–H), 1683 (C=O), 1585, 1515 (C=N/aromatic C=C), 1276, 1194, 1111, 1031 (C–O/C–N), 852, 794, 746 (aromatic C–H bending).

The IR spectrum of DHPT1 showed characteristic absorption bands supporting the proposed structure. Bands at 3411 and 3170 cm^{-1} were attributed to O–H and N–H stretching, respectively, while the absorption at 2998 cm^{-1} corresponded to aliphatic C–H stretching. A prominent band at 1683 cm^{-1} indicated ester C=O stretching. Absorptions at 1585 and 1515 cm^{-1} were assigned to C=N and aromatic ring vibrations. Bands in the fingerprint region corresponded to C–O, C–N, and C=S-related vibrations, consistent with the proposed structure.

3166 (N–H), 2923, 2851 (aliphatic C–H), 1703 (C=O), 1632, 1612, 1575, 1520 (C=N/aromatic C=C), 1242,

1126, 1007 (C–O/C–N), 787, 740 (aromatic C–H bending).

The IR spectrum of DHPT2 exhibited characteristic absorption bands supporting the proposed structure. The band at 3167 cm^{-1} was attributed to N–H stretching, while absorptions at 2923 and 2852 cm^{-1} corresponded to aliphatic C–H stretching. A prominent band at 1703 cm^{-1} indicated ester C=O stretching. Bands at 1631, 1611, 1574, and 1520 cm^{-1} were associated with C=N and aromatic ring vibrations. Absorptions in the fingerprint region were attributed to C–O, C–N, and C=S-related vibrations, consistent with the proposed structure.

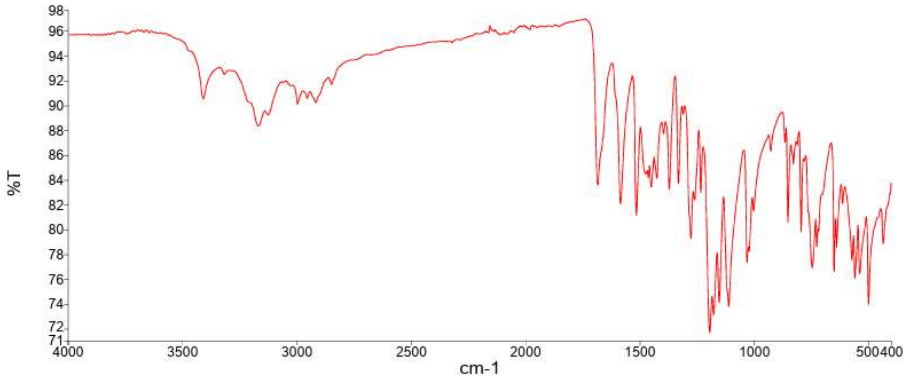

Figure 13: IR Spectrum of DHPT1

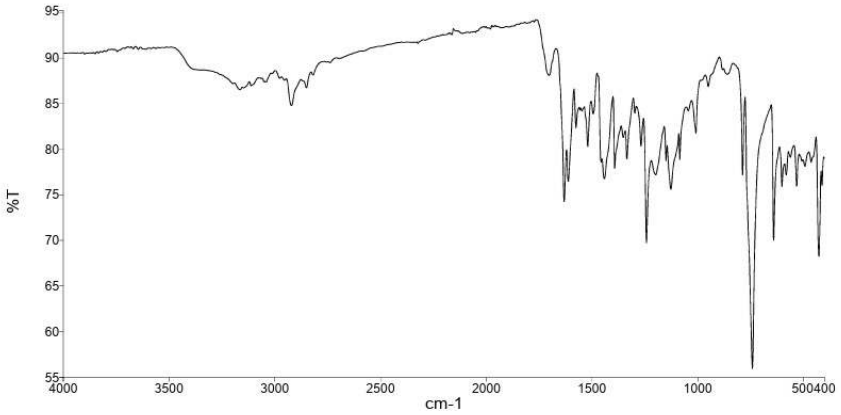

Figure 14: IR Spectrum of DHPT2

3.2 PHARMACOKINETIC STUDY BY SWISSADME

Table 1: Pharmacokinetic Study by SwissADME

COMPOUND	PHARMACOKINETIC PROPERTIES
DHPT1	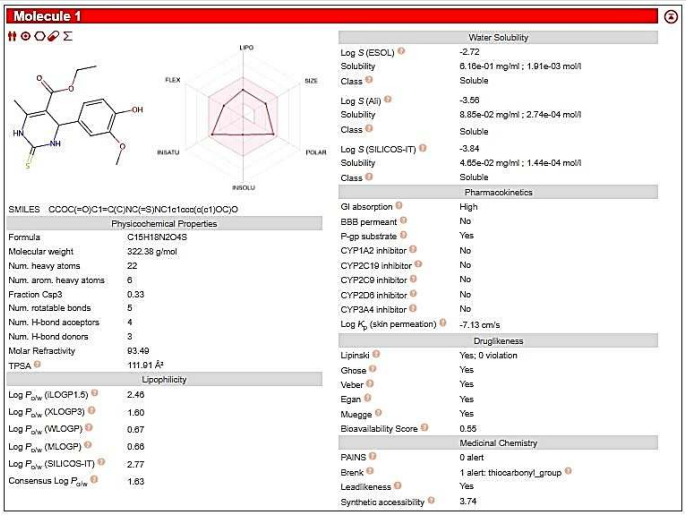
DHPT2	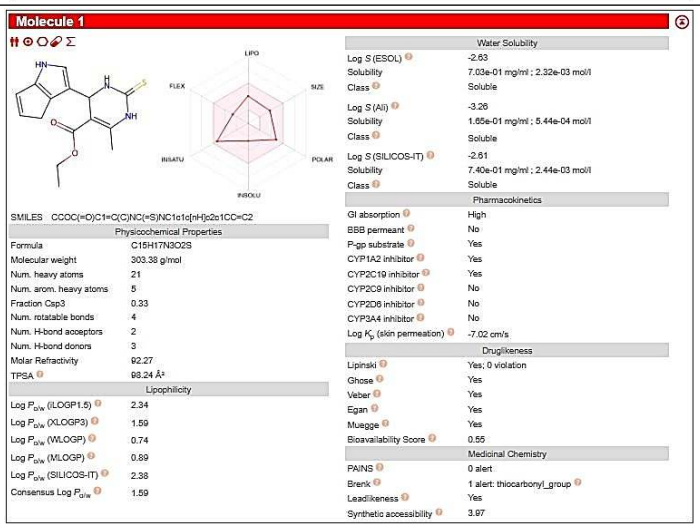
DHPT3	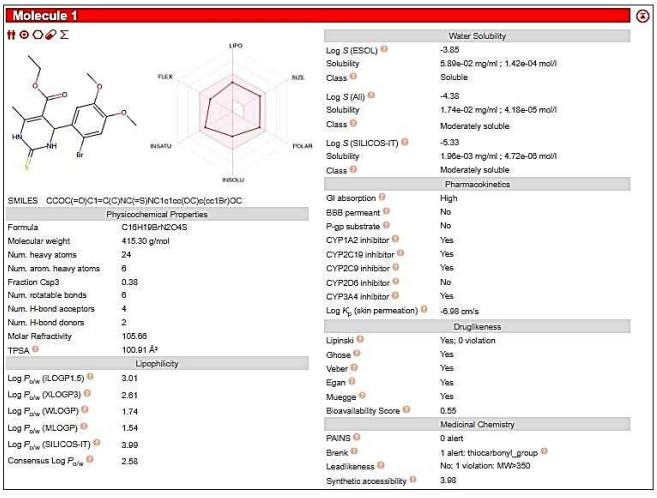

COMPOUND	PHARMACOKINETIC PROPERTIES
DHPT4	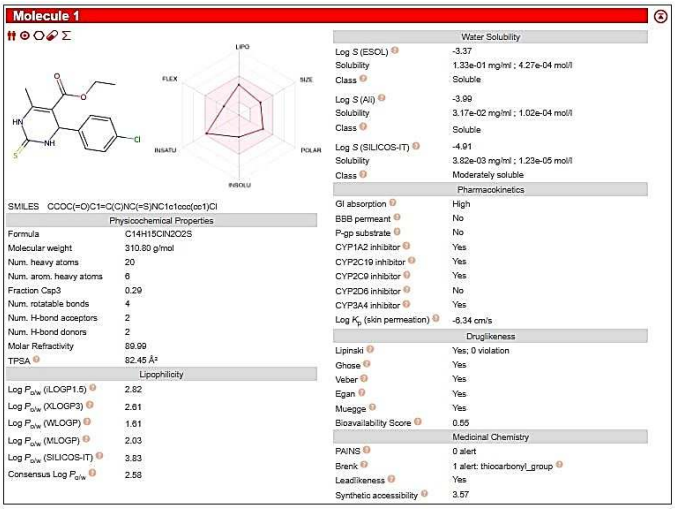

Table 2: Lipsinki's Rule of Five Analysis of DHPMT Derivatives Using SwissADME

COMPOUND	MOLECULAR WEIGHT(g/mol)	HBA	HBD	Consensus Log P	Lipsinki Violation
DHPT1	322.38	4	3	1.63	0
DHPT2	303.38	2	3	1.59	0
DHPT3	415.30	4	2	2.58	0
DHPT4	310.80	2	2	2.58	0
DHPT5	388.26	3	3	2.38	0
DHPT6	389.70	2	2	3.15	0
DHPT7	373.24	3	2	3.00	0
DHPT8	389.70	2	2	3.21	0
DHPT9	306.38	3	2	2.10	0
DHPT10	308.35	4	4	1.20	0

3.3 In-silico TOXICITY PREDICTION – Protox.3.0

Table 3: Toxicity Prediction by PROTOX.3.0

COMPOUND	PROTOX TOXICITY
DHPT1	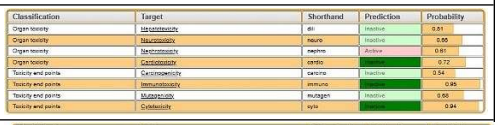
DHPT2	
DHPT3	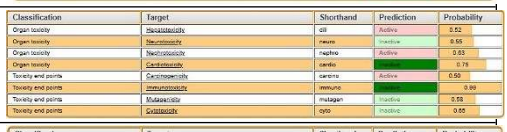
DHPT4	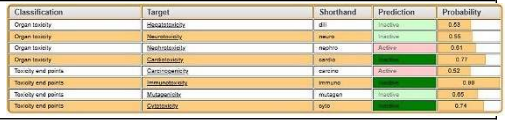

3.4 DOCKING RESULTS

The designed molecules underwent docking against selected protein (PDB ID:1KE9 ,1ZYX) and the compounds were filtered and sorted based on their respective docking score. The most favourable and stable pose was selected based on the docking score and multiple interactions observed. Among the docked molecules, DHPT1 exhibit the highest binding affinity towards the protein 1KE9, while DHPT6 demonstrate the lowest binding affinity and in case of protein 1ZYX, DHPT2 exhibit highest binding affinity, DHPT6 demonstrate the lowest binding affinity.

Table 4: Docking Results

Sl. no	Compound	Structure	Docking Score	
			1KE9	1ZYX
1	**DHPT1**	Ethyl 4-(4-hydroxy-3-methoxyphenyl)-6-methyl-2-thioxo-1,2,3,4-tetrahydropyrimidine-5-carboxylate	-7.5	-7.5
2	**DHPT2**	Ethyl 4-(1*H*-indol-3-yl)-6-methyl-2-thioxo-1,2,3,4-tetrahydropyrimidine-5-carboxylate	-7.3	-7.8
3	**DHPT3**	Ethyl 4-(2-bromo-4,5-dimethoxyphenyl)-6-methyl-2-thioxo-1,2,3,4-tetrahydropyrimidine-5-carboxylate	-6.8	-7.3
4	**DHPT4**	Ethyl 4-(chlorophenyl)-6-methyl-2-thioxo-1,2,3,4-tetrahydropyrimidine-5-carboxylate	-6.9	-7.2
5	**DHPT5**	Ethyl 4-(5-amino-4-bromo-2-flurophenyl)-6-methyl-2-thioxo-1,2,3,4-tetrahydropyrimidine-5-carboxylate	-6.4	-7.2
6	**DHPT6**	Ethyl 4-(2-bromo-5-chlorophenyl)-6-methyl-2-thioxo-1,2,3,4-tetrahydropyrimidine-5-carboxylate	-6.2	-6.9
7	**DHPT7**	Ethyl 4-(3-bromo-2-flurophenyl)-6-methyl-2-thioxo-1,2,3,4-tetrahydropyrimidine-5-carboxylate	-6.4	-6.5
8	**DHPT8**	Ethyl 4-(5-bromo-2-chlorophenyl)-6-methyl-2-thioxo-1,2,3,4-tetrahydropyrimidine-5-carboxylate	-6.1	-6.4
9	**DHPT9**	Ethyl 4-(4-methoxyphenyl)-6-methyl-2-thioxo-1,2,3,4-tetrahydropyrimidine-5-carboxylate	-6.1	-6.3
10	**DHPT10**	Ethyl 4-(3,4-dihydroxyphenyl)-6-methyl-2-thioxo-1,2,3,4-tetrahydropyrimidine-5-carboxylate	-5.4	-5.8

Table 5: Interacting Residues of DHPT1 and DHPT2

COMPOUND	INTERACTING RESIDUE	
	1KE9	1ZYX
DHPT1	GLU A:12 ILE A: 10 GLN A: 131 ASP A: 36	ALA A:18 LEU A:2 PHE A:5
DHPT2	LEU A:202 ARG A:214 THR A:218 ARG A:217 GLN A:246	ALA A:18 SER A:23 HIS A:48 TYR A:52 LEU A:2 LYS A:69

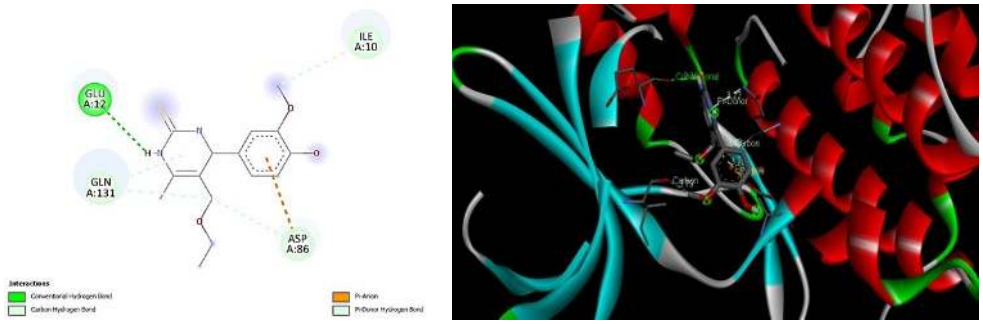

Figure 15: (A) Binding Interaction of DHPT1 with 1KE9, (B) Binding Pattern of DHPT1 with 1KE9 in Binding Pocket.

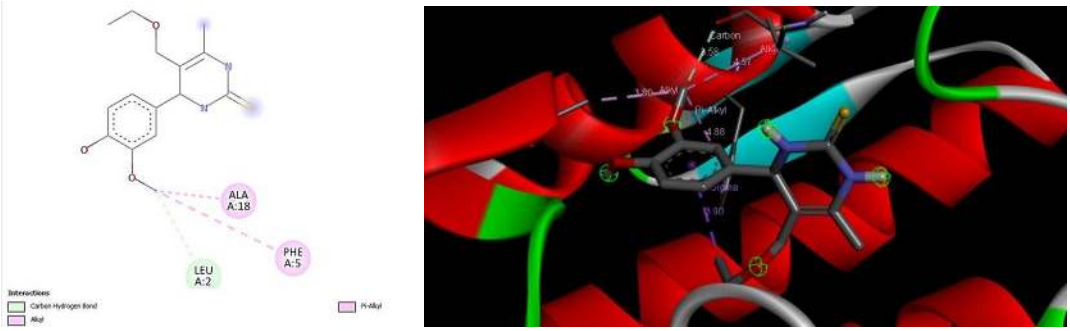

Figure 16: (a) Binding interaction of DHPT1 with 1ZYX, **(b)** Binding pattern of DHPT1 with 1ZYX in binding pocket.

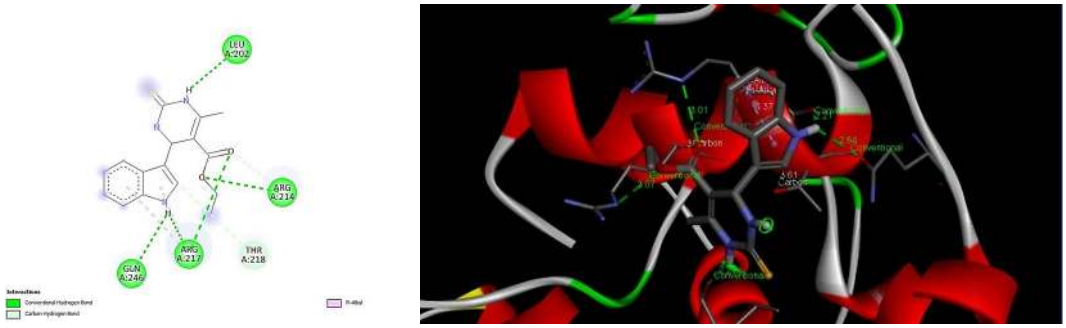

Figure 17: (A) Binding Interaction of DHPT2 with 1KE9, (B) Binding Pattern of DHPT2 with 1KE9 in Binding Pocket.

.

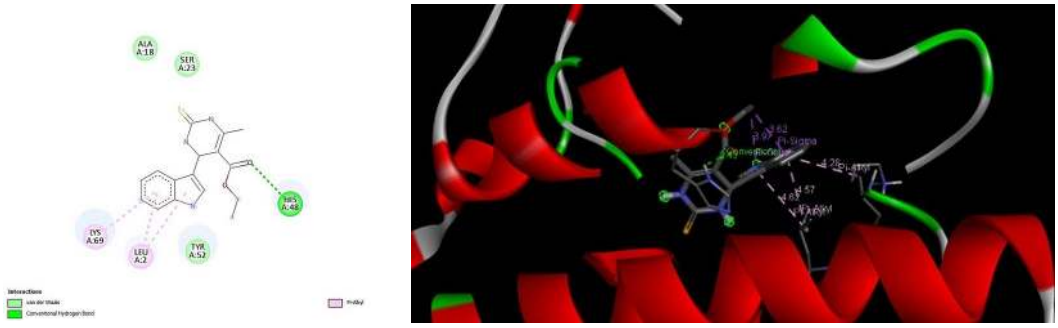

Figure 18: (A) Binding Interaction of DHPT2 with 1ZYX, (B) Binding Pattern of DHPT2 with 1ZYX in Binding Pocket.

3.5 BIOLOGICAL EVALUATION

HRBC membrane stabilization method

The *in vitro* HRBC membrane stabilization assay was performed to evaluate the anti-inflammatory potential of DHPT1 and DHPT2, using indomethacin as the standard drug. Both compounds exhibited concentration-dependent inhibition of haemolysis, indicating their potential to stabilize the erythrocyte membrane. Indomethacin exhibited membrane stabilization of 74.67% at 100 µg/mL, DHPT1 and DHPT2 exhibited membrane stabilization of 70.22% and 71.57% respectively. Although DHPT2 exhibited slightly higher membrane stabilization than DHPT1, its activity was moderate when compared with indomethacin. The IC_{50} values of DHPT2, DHPT1, and indomethacin were 18.20 µg/mL, 26.72 µg/mL, and 14.88 µg/mL respectively. These findings suggest that DHPT2 demonstrated promising in vitro membrane-stabilizing activity.

Table 6: Effect of DHPT1, DHPT2 and Standard Drug on HRBC Membrane Haemolysis and Membrane Stabilization.

Compound	Concentration (µg/ml)	Absorbance (nm)	%Haemolysis	%Stabilization	IC50 (/)
Indomethacin	10	0.950	64.14	35.85	14.88
	20	0.521	35.17	64.82	
	50	0.481	32.47	67.52	
	100	0.375	25.32	74.67	
DHPT1	10	0.930	62.79	37.20	26.72
	20	0.820	55.36	44.63	
	50	0.465	31.39	68.60	
	100	0.441	29.77	70.22	
DHPT2	10	0.925	62.45	37.54	18.20
	20	0.700	47.26	52.73	
	50	0.556	37.54	62.45	
	100	0.421	28.42	71.57	

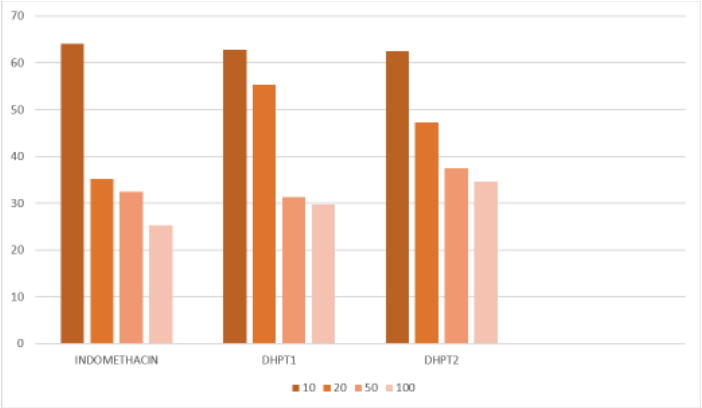

Figure 19: Effect of Standard,DHPT1 & DHPT2 on HRBC Membrane Haemolysis

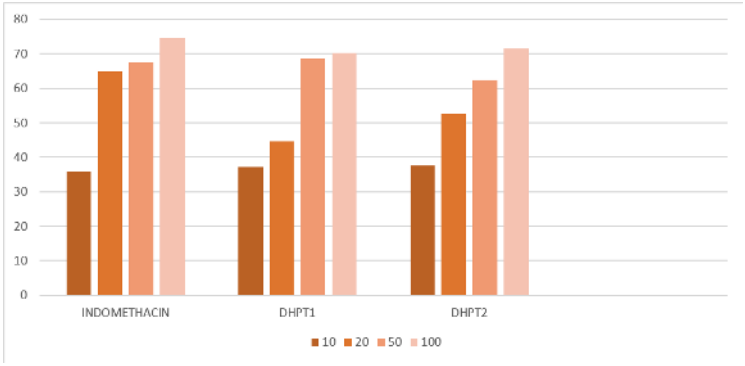

Figure 20: Effect of Standard,DHPT1 & DHPT2 on HRBC Membrane Stabilization

MTT assay

The compound with the highest docking score (DHPT1) was selected for *in-vitro* studies. To assess its cytotoxic activity against the MCF7 breast cancer cell line, the MTT assay was employed. This colorimetric assay relies on the reduction of a yellow tetrazolium salt known as MTT (3-(4,5-dimethylthiazol-2-y1)-2,5-diphenyltetrazolium bromide) to form purple formazan crystals by metabolically active cells. The presence of NAD (P)H-dependent oxidoreductase enzymes in viable cells facilitates the reduction of MTT to formazan. The insoluble formazan crystals are subsequently dissolved using 100% DMSO (a solubilizing solution), and the resulting purple-colored solution is quantified by measuring absorbance at 570 nm using an ELISA plate reader. By analyzing the optical density, the percentage viability and IC_{50} values were calculated.

Table 7: MTT Assay Results for Varying Concentration of DHPT1

Concentration of DHPT1(µg/ml)	Triplicate values			Average OD
	OD1	OD2	OD3	
Control	0.806	0.802	0.817	0.808
6.25	0.800	0.796	0.802	0.799
12.5	0.769	0.776	0.774	0.773
25	0.725	0.723	0.728	0.725
50	0.650	0.655	0.642	0.649
100	0.522	0.504	0.501	0.509

Table 8: Percentage of Viability for Varying Concentration of DHPT1

Concentration (µg/ml)	Percentage of viability
6.25	98.89
12.5	95.63
25	89.73
50	80.29
100	62.97
IC_{50}	>100 µg/ml

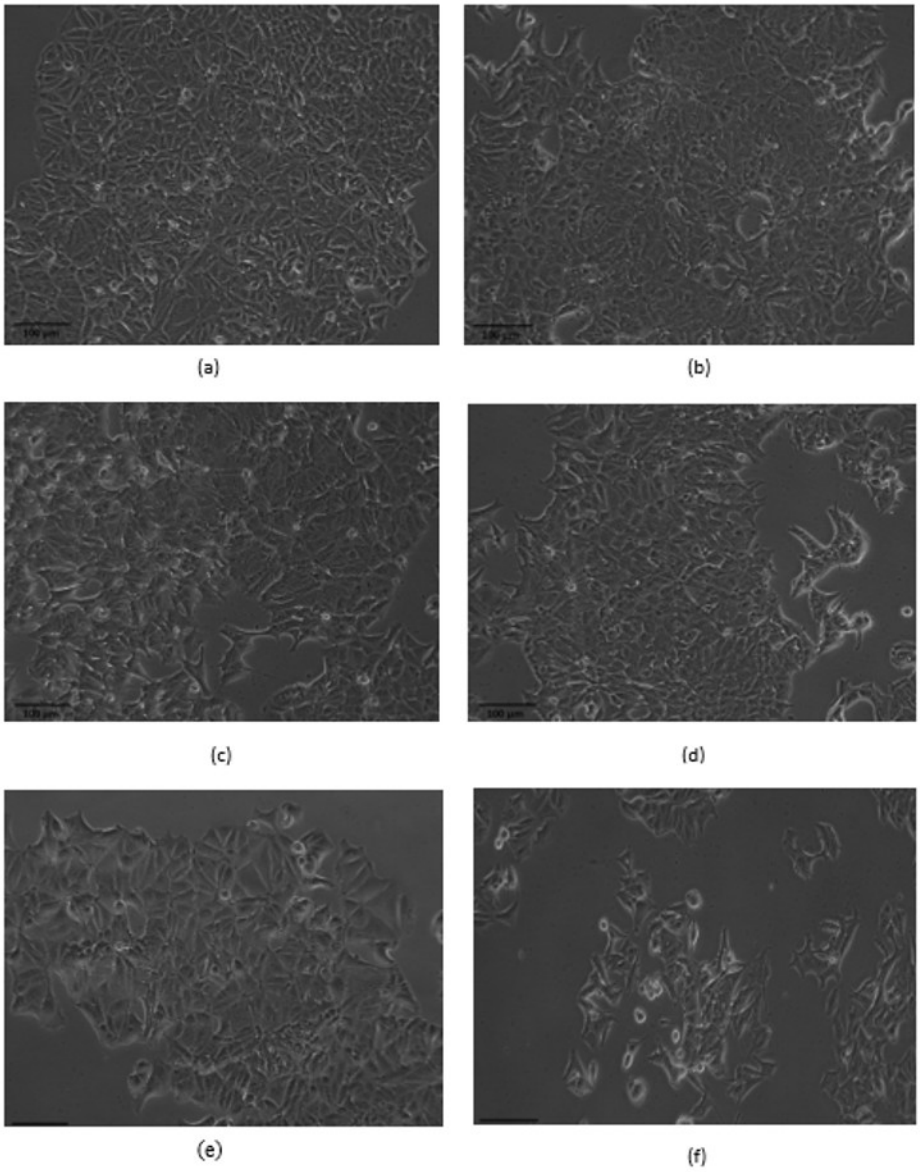

Figure 21: Microscopic Image of MCF7 Cell Treated with Different Concentration of DHPT1

(a)control, (b) 6.25, (c)12.5, (d)25, (e)50 and (f)100 (µg/ml)

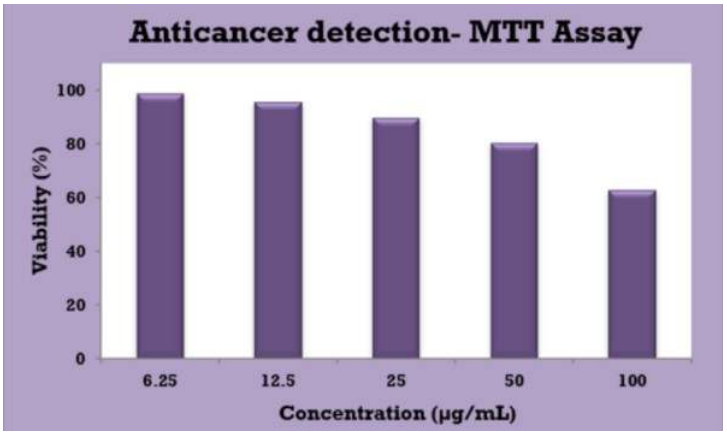

Figure 22: Graphical Representation

A dose-dependent reduction in cell viability was observed in MCF-7 cancer cells treated with different concentrations of the sample. Maximum cytotoxicity was observed at 100 µg/mL, with approximately 63% cell viability. As cell viability remained above 50% at the highest tested concentration, the IC_{50} value could not be reliably determined within the tested concentration range. Further testing at higher concentrations is required.

ACKNOWLEDGEMENT

At this moment of accomplishment, we would like to express our sincere thanks to our guide **Nivea Cleo T S**, Associate professor in Department of Pharmaceutical Chemistry, Crescent College of Pharmaceutical Sciences for her valuable guidance and encouragement throughout the research work and the successful completion of our project work.

We would like to express our sincere gratitude to **Dr Suja C**, Principal and **Dr Sreena K**, Vice Principal and HOD Department of Pharmaceutical Chemistry, Crescent College of Pharmaceutical Sciences for their valuable help and providing necessary facilities to carry out this work.

CONFLICT OF INTEREST

We declare that we have no conflict of interest.

REFERENCES

1. Nag S, Ghosh A, Mitra S, Dasgupta S. Lifestyle and reproductive factors associated with breast cancer risk: a review. Clin Epidemiol Glob Health. 2023;19:101215.
2. Patro VJ, Sheela E, Srinavya M, Jyothika A, Sailaja M. A review on pathophysiology of breast cancer. Int J Pharm Sci Drug Anal. 2023;3 (1):94-7.
3. Burdall SE, Hanby AM, Lansdown MR, Speirs V. Breast cancer cell lines: friend or foe? Breast Cancer Res. 2003;5:89-95.
4. Anait S and Jordan VC (1997), 'MCF-7: the first hormone-responsive breast cancer cell line', Cancers, 57:3 071-8.
5. Furman D, Campisi J, Verdin E, et al. Chronic inflammation in the etiology of disease across the life span. Nat Med. 2019;25 (12):1822-32.
6. Loane DJ, Kumar A. Microglia in the TBI brain: the good, the bad, and the dysregulated. Exp Neurol. 2016;275:316-27.
7. Muheyuddeen G, Khan MY, Ahmad T, et al. Design, synthesis, and biological evaluation of novel imidazole derivatives as analgesic and anti-inflammatory agents: experimental and molecular docking insights. Sci Rep. 2024;14:23121.
8. Alshuweishi Y, Abudawood A, Alfayez D, Almufarrih AA, Alanazi F, Alshuweishi FA, et al. Platelet/high-density lipoprotein ratio (PHR) predicts type 2 diabetes in obese patients: a retrospective study. Healthcare (Basel). 2024;12:1540.
9. Avelyev A, Khrustalev D, Losseva I, Yedrissov A, Khrustaleva A, Sofiya S, et al. Structural and functional aspects of DHPM-thiones and their derivatives: a critical review of pharmaceutical potential. Pharmaceuticals (Basel). 2026 Feb 12;19 (2):306.
10. Matos LHS, Masson FT, Simeoni LA, Homem-de-Mello M. Biological activity of dihydropyrimidinone (DHPM) derivatives: a systematic review. Eur J Med Chem. 2018;143:1779-89.
11. Sheik Mansoor S, Syed Shafi S, Zaheer Ahmed S. An efficient one-pot multicomponent synthesis of 3,4-dihydropyrimidine-2-(1H)-ones/thiones/ imines via a Lewis base catalyzed Biginelli-type reaction under solvent-free conditions. Arab J Chem. 2016;9 (Suppl).
12. Daina A, Michielin O, Zoete V. SwissADME: a free web tool to evaluate pharmacokinetics, drug-likeness and medicinal chemistry friendliness of small molecules. Sci Rep. 2017;7:42717.
13. Lipinski CA, Lombardo F, Dominy BW, Feeney PJ. Experimental and computational approaches to estimate solubility and permeability in drug discovery and development settings. Adv Drug Deliv Rev. 2001;46 (1-3):3-26.
14. Banerjee P, Kemmler E, Dunkel M, Preissner R. ProTox 3.0: a webserver for the prediction of

toxicity of chemicals. Nucleic Acids Res. 2024;52 (W1).

15. Parasuraman S. Prediction of activity spectra for substances. J Pharmacol Pharmacother. 2011;2 (1):52-3.
16. Trott O, Olson AJ. AutoDock Vina: improving the speed and accuracy of docking with a new scoring function, efficient optimization, and multithreading. J Comput Chem. 2010;31 (2):455-61.
17. Eberhardt J, Santos-Martins D, Tillack AF, Forli S. AutoDock Vina 1.2.0: new docking methods, expanded force field, and Python bindings. J Chem Inf Model. 2021;61 (1):389-98.
18. Rauf MA, Zubair S, Azhar A. Ligand docking and binding site analysis with PyMOL and AutoDock/Vina. Int J Basic Appl Sci. 2015;4 (2):168-77.
19. Seeliger D, de Groot BL. Ligand docking and binding site analysis with PyMOL and AutoDock/Vina. J Comput Aided Mol Des. 2010;24 (5):417-22.
20. Pawar RP, Rohane SH. Role of AutoDock Vina in PyRx molecular docking. Asian J Res Chem. 2021;14 (2):132-4.
21. Shamna Z, Greeshma S, Sumathy A, Gowrishankar NL. Synthesis of Schiff bases of indole-3-carboxaldehyde derivatives using Biginelli reaction and their antioxidant evaluation. Int J Pharm Sci. 2024;2 (10):218-23.
22. Yalkowsky SH, Alantary D. Estimation of melting points of organics. J Pharm Sci. 2018;107 (5):1211-27.
23. Neto BAD, Beck PS, Sorto JEP, Eberlin MNE. In melting points we trust: a review on the misguiding characterization of multicomponent reactions adducts and intermediates. Molecules. 2022;27 (21):7552.
24. Sakat S, Juvekar AR, Gambhire MN. In-vitro antioxidant and anti-inflammatory activity of methanol extract of Oxalis corniculata Linn. Int J Pharm Pharm Sci. 2010;2 (1):146-55.
25. Mosmann T. Rapid colorimetric assay for cellular growth and survival: application to proliferation and cytotoxicity assays. J Immunol Methods. 1983;65:55-63.
26. Joseph MM, Aravind SR, Varghese S, Mini S, Sreelekha TT. Evaluation of antioxidant, antitumor and immunomodulatory properties of polysaccharide isolated from fruit rind of Punica granatum. Mol Med Rep. 2012;5 (2):489-496.

HOW TO CITE: Nivea Cleo Ts, Sreena K., Fathima Rifa P., Fathima CT, Fathimath Rasha Vv, Akshaya Gp, In Silico Design, Synthesis, Characterization and Bioactivity Profiling of Dihydropyrimidine-2-Thione Derivatives, Int. J. of Pharm. Sci., 2026, Vol 4, Issue 11, 5258-5277. https://doi.org/10.5281/zenodo.24578615